Journal of Applied Polymer Science

Investigation of Membrane Preparation Condition Effect on the PSD and Porosity of the Membranes Using a Novel Image Processing Technique

Ashkan Zolfaghari Sharak, Armin Samimi, Seyyed Abbas Mousavi, Ramin Bozorgmehri Bozarjamhari
Chemical and Petroleum Engineering Department, Sharif University of Technology, Azadi Av., Tehran, Iran
Correspondence to: S. A. Mousavi (E-mail: musavi@sharif.edu)

ABSTRACT: A totally computerized image processing program package is developed to analyze the SEM images of membrane surface and cross-section. Pore size distribution and porosity of the fabricated membranes are determined using the proposed image processing procedure. Furthermore, effect of coagulation bath temperature on the morphology and mechanical properties (such as tensile strength, strain break, tensile energy absorbent, and tensile stiffness) of Polysulfone (PSf) membranes are investigated. The results reveal that the mechanical properties are higher when *N*-methyl-2-pyrrolidone (NMP) is used as solvent. Also, an increase in the coagulation bath temperature caused a monotonous increase in the mean pore size value of Dimethylformamide (DMF)-based membranes. However, mean pore size curve has a maximum when NMP is used as solvent. Also, porosity of the fabricated membranes increased when coagulation bath temperature increased. For the NMP-base membranes, pore's diameter was in the range of 0–5 μm. However, DMF-based membranes have pore size value of smaller than 1 μm when the precipitation medium is kept at 8°C. © 2013 Wiley Periodicals, Inc. J. Appl. Polym. Sci. **2014**, *131*, 39899.

KEYWORDS: image processing; membranes; morphology; porous materials

Received 14 December 2012; accepted 27 August 2013
DOI: 10.1002/app.39899

INTRODUCTION

Nowadays polymeric membranes are used for many applications such as gas–liquid separation, ultrafiltration, microfiltration, and pharmacy.[1] Common way of preparing such membranes is phase inversion method that a thin layer of polymeric solution is casted on a support and then solvent is removed from the solution.[2] There are two methods for fabrication of membranes: wet and dry phase inversion. Dry phase inversion occurs with evaporation of volatile solvent or dissolution within the air moisture as the non-solvent. Wet phase inversion executes by floating of the polymeric solution film in the coagulation bath of non-solvent. The solvent and the non-solvent are exchanged with each other, and the polymeric membrane forms. Polysulfone (PSf) is one of the membranes which form withthe phase inversion method. High mechanical and thermal properties and good resistance in acidic environment are the main properties of PSf that made it suitable for fabrication of polymeric membranes.[3] Final structure and the properties of PSf membranes are strongly depend on the experimental parameters such as composition of polymeric solutions, coagulation bath temperature, supporting materials, and the temperature of the dope solution.

The effects of operational parameters and process variables on the membrane morphology were investigated by many researchers. Numbers of these efforts are focused on the effect of solvent and non-solvent type on the membrane properties.[3–9] Kaiser et al.[3] studied the morphology of the PSf membrane which was prepared by wet phase inversion method in the ternary system of PSF/DMA/Water. Madaeni et al.[4] investigated the effect of different solvent such as NMP, DMF, and DMA on morphology and performance of UF PSf. The effect of different solvent on the properties of SPES membranes were studied by Guan et al.[5] They showed that casting solvents have strong effects on the morphology and performance of SPES membranes.

Other studies focused on how the membrane structure affected by additives and fabrication condition.[10–22] Chakrabarty et al.[10,20] worked on performance and properties of PSf membrane by adding PVP and PEG to the dope solution. Their results reveal that number of pores and pore surface increase with an increase in the molecular weight of the additives. The effect of additives and preparation conditions on the morphology of cellulose acetate membranes were studied by Mohammadi et al.[11–14] They presented the water permeability within the fabricated membranes to show the morphology differences. Aroona et al.[15] investigated the effects of polymeric additives concentration, the concentration of polymer within the dope solution, and non-solvent type on structure and performance of the flat sheet PSf membranes. They revealed that

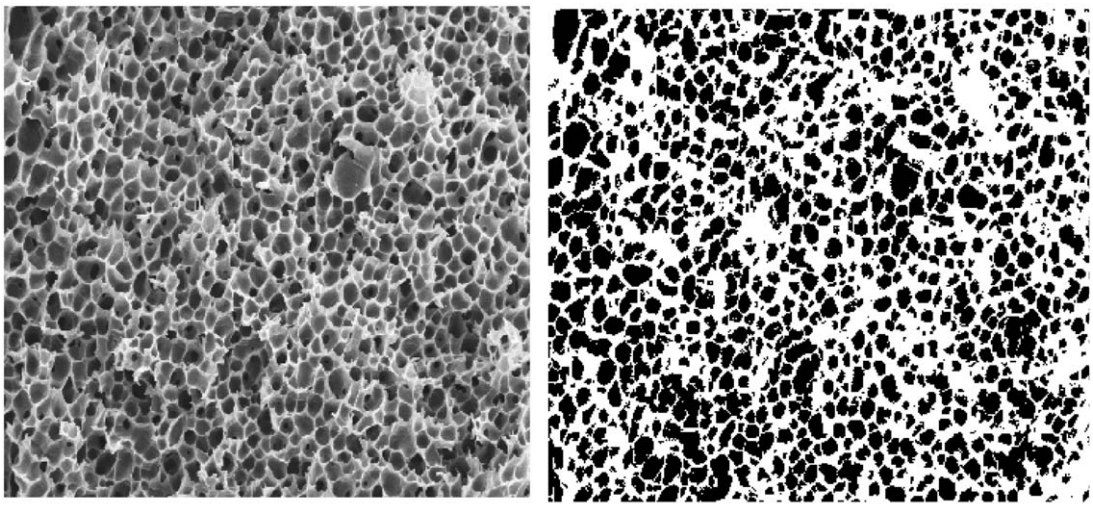

Figure 1. Pore extraction of the membrane cross-section: (a) The original SEM image; (b) Binary image of the membrane. The black regions are pore space while the white parts represent the membrane solid structure.

the separation properties of the membranes are improved by presence of additives. Chen et al.[16] studied the effect of solvent polarity on the membrane formation in ternary system of PSf/NMP/Water. Barth et al.[17] made inquiry onto the effects of thermodynamic conditions on structure of the asymmetric PSf membranes. Sobhanipour et al.[18] investigated the coagulation bath temperature effect on the morphology of polyacrylonitrile fibers. Barzin et al.[19] led an experiment on the influences of preparation conditions on morphology and performance of hemodialysis membranes.

Pore size and pore size distribution (PSD) are particularly important in respect of transport phenomena within the structure and mechanical properties of the membranes. Several methods had been proposed to determine mean pore size and PSD in porous materials. For instance, Yang and Manthiram[23] use the small angle X-ray scattering method to study the microstructural evolution and swelling behaviors of sulfonated poly(etheretherketone) and Nafion polymer membranes. Bowen and Doneva applied a fast Fourier transform filtering to remove the image's noise in the atomic force microscope images of the membranes.[24] Zhao et al.[25] reviewed different methods to characterize the mean pore size and the pore size distribution of porous hollow fiber membranes. Sun et al.[26] developed a digital image processing program package to calculate the porosity, and pore diameter distribution of membrane surface by treating the SEM photos of membrane surface and cross-section. They used a human–computer interactive system to resolve the contrast intensification problem of the SEM images.

Effects of various additives and preparation conditions on the pore size and PSD were investigated by many researchers. For instance, effect of air humidity on the membrane morphology and PSD was studied by Matsuyama et al.[27] The impact of production conditions on the PSD of membrane bioreactors (MBR) and its effects on the filtration performance of submerged hollow fibers was investigated by Buetehorna et al.[28] Effect of various additives (such as 1, 4-dioxane, DGDE, acetone, and GBL) on the pore size of PSf membrane was studied by Kim and Lee.[29]

In the past, the micrographs were taken manually by ImageJ program or it is predicted using a human–computer interactive system. In such procedures, the human errors could affect the final results. However, in this study, a totally computerized image processing program package was developed to analyze the SEM images of the membranes. The predicted PSDs are used to study the effect of coagulation bath temperature and type of solvent on the morphology and mechanical properties of the fabricated PSf membranes.

EXPERIMENTAL

Materials

Polysulfone supplied by BASF (PSf; Ultrason® S 6010) was used to prepare the membranes. *N*-Methyl-2-pyrrolidone (NMP; purity: 99.5%) and Dimethylformamide (DMF; purity: 99.5%) were purchased from Merck. NMP and DMF were used as two different solvents and deionized water was applied as non-solvent in the coagulation bath.

Membrane Preparation Method

Wet phase inversion method was used for fabrication of the membranes. Solutions of 20% of PSf in NMP or DMF were used as the casting medium. The casting solutions were stirred for 1 day and were dispersed on a smooth glass support by a doctor blade in the room temperature. Polymer solution films were immediately precipitated in the coagulation bath containing distilled water as the non-solvent. The coagulation bath temperature was fixed in three different values of 8, 25, and 57°C. To complete the phase inversion process, the polymer films were kept in the water bath for 24 h. Then the fabricated membranes were dried in the room temperature for another 24 h.

Scanning Electron Microscopy Photographs

The membranes morphology was observed with a JSM-5800 scanning electron microscopy (SEM). The observations were carried out on the cross-section of the membranes broken in liquid nitrogen and coated with gold by sputtering.

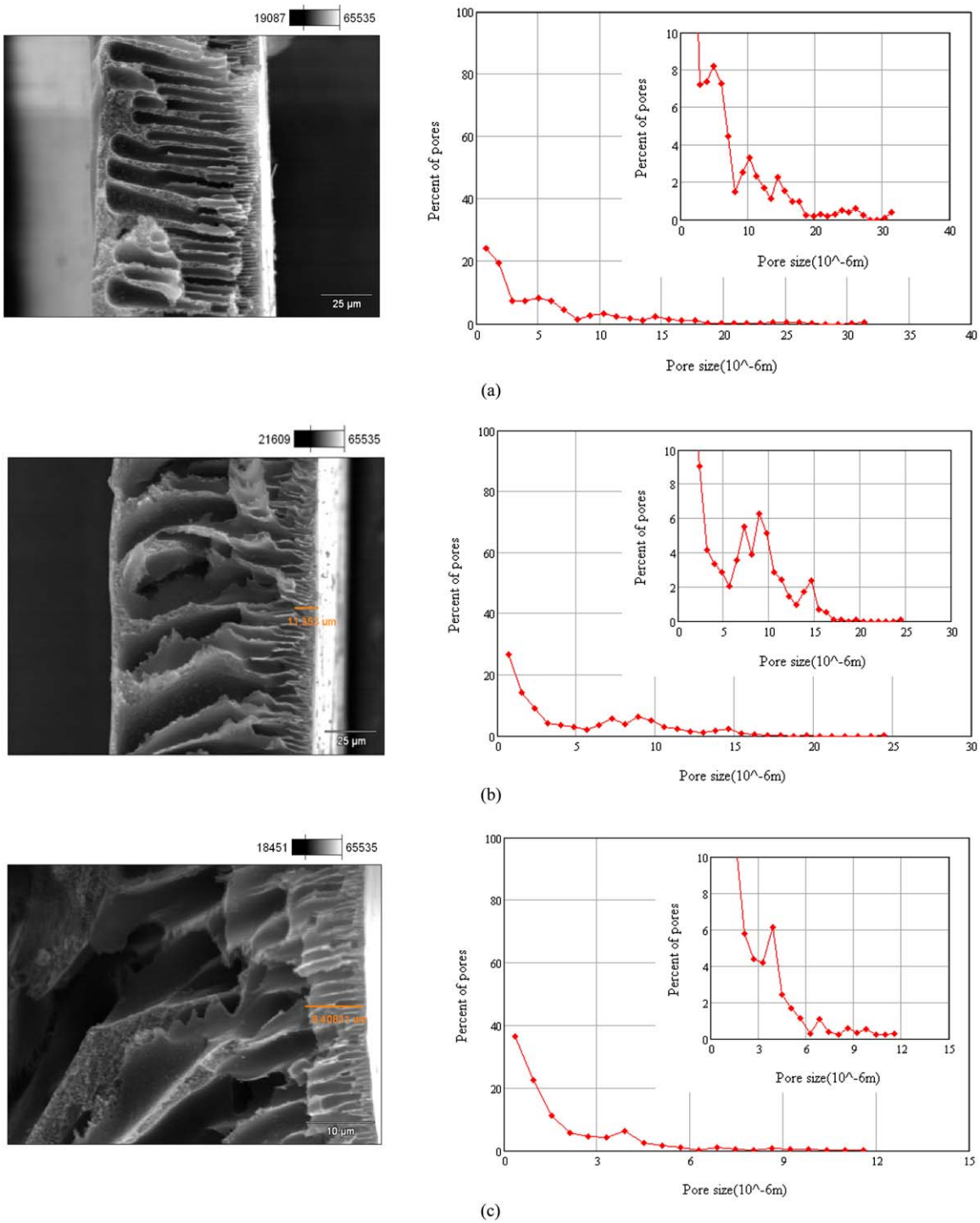

Figure 2. SEM image and PSD of 20% PSf of membranes in NMP at (a) 57°C, (b) 25°C, and (c) 8°C. [Color figure can be viewed in the online issue, which is available at wileyonlinelibrary.com.]

METHODOLOGY

Mean Pore Size Calculations

In this study, a totally computerized method is used to calculate the PSD from the SEM images. The mean pore size of the prepared membranes was determined by the method presented by Deshmukh and Li[30]:

$$m=(16B_0/3P_0)(2RT/\pi M)^{1/2} \quad (1)$$

where m is the mean pore size (cm), B_0 is geometry factor of porous media (cm^2), P_0 is Knudsen permeability coefficient (cm^2/s), and M is molecular weight of the permeate. B_0 and P_0 values can be obtained from the gas permeability coefficient data:

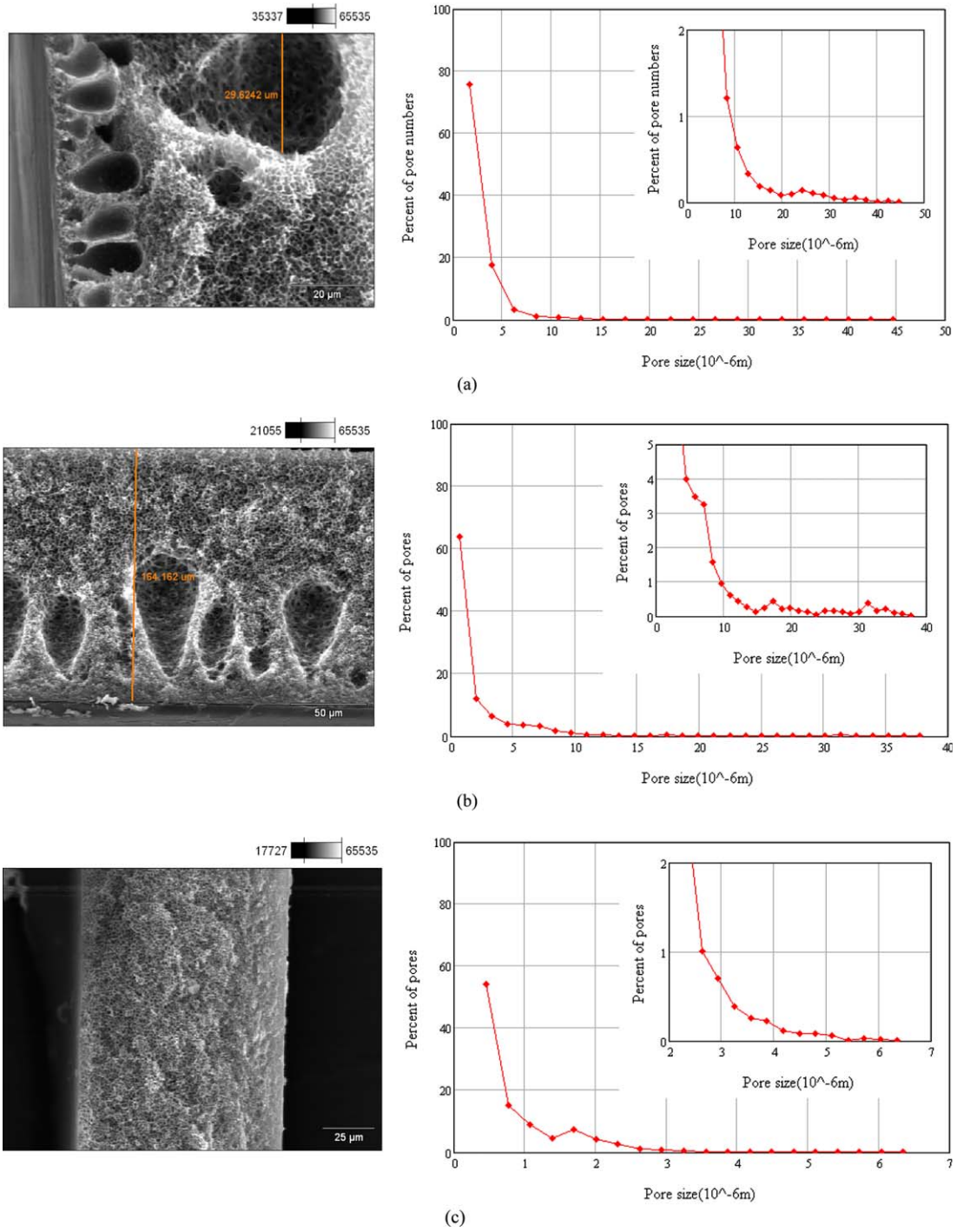

Figure 3. PSD of 20% PSf of membranes in DMF at (a) 57°C, (b) 25°C, and (c) 8°C. [Color figure can be viewed in the online issue, which is available at wileyonlinelibrary.com.]

$$P = P_0 + (\Delta P^*/\mu) g_0 \quad (2)$$

$$\Delta P^* = (P_1 + P_2)/2 \quad (3)$$

where P_1 and P_2 are the upstream and downstream pressures (dyn/cm^2), μ is the permeate viscosity (dyn s/cm^2). P can be determined by gas permeability test in different pressures:

$$P = LP^*Q/A\Delta P \quad (4)$$

where L is the membrane thickness (cm), P^* is the discharged pressure, ΔP is the pressure difference across the membrane, A is the membrane surface (cm^2), and Q represents the permeation flux (cm^3/s). The calculated mean pore size is used as the adjustable parameter to fix the binary image contrast.

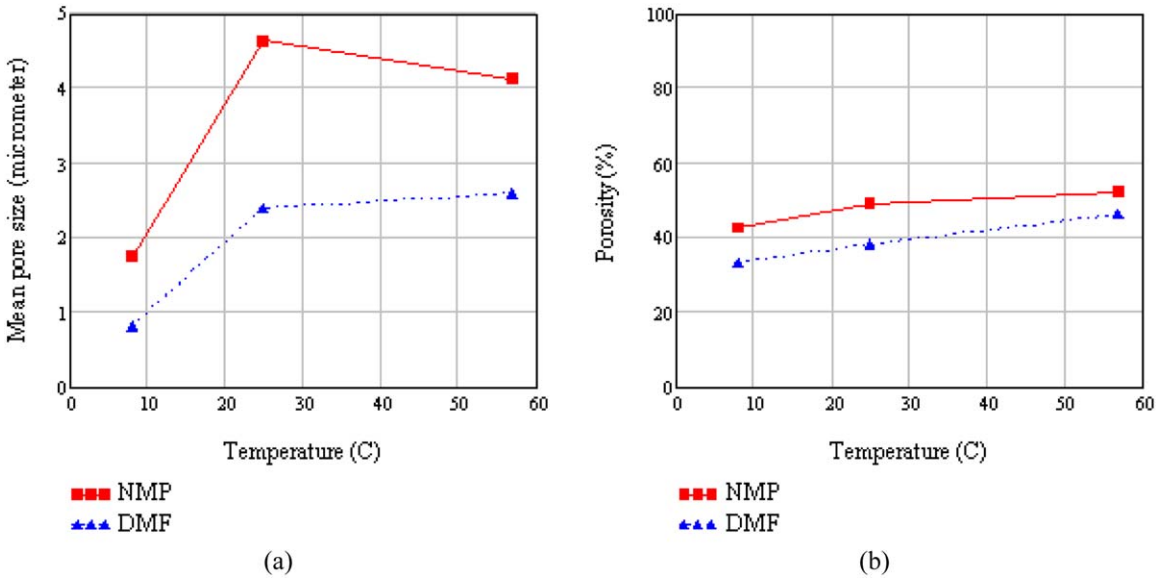

Figure 4. (a) Mean pore size and (b) calculated porosity of 20% of PSf membranes in DMF and NMP at 8, 25, and 57°C. [Color figure can be viewed in the online issue, which is available at wileyonlinelibrary.com.]

Image Processing

In a color image, each pixel is determined by three numbers between 0 and 255, which give the amount of red, green, and blue which are combined to make the pixel's color. However, in a gray scale image the pixel values are numbers between 0 (black) and 255 (pure white). Therefore, in our image processing program package, the SEM images were binarized to the values of 0 or 255 (black and white) and then analyzed using the program to find the precise pore size distribution.

The cross-section of the prepared membranes was inspected with the JSM-5800 scanning electron microscope (SEM). The contrast of images is intensified from 0 to 255. A binary image is generated to distinguish between the pore space and the membrane solid structure. Figure 1 represents an SEM image of the membrane cross-section and the generated binary image.

As it is mentioned before, Sun et al.[26] applied a human–computer interactive system to deal with the contrast intensification of the SEM images. They used a manual threshold to remove the image's noise. To the best of our knowledge, in all available image processing procedures the image contrast (brightness) is controlled manually. However, the novelty of our work is that the image contrast is automatically estimated using the augmented SEM images of the membrane cross-section and the experimental data of the mean pore size.

In this article, an image processing program package is developed to find the most fitted threshold using the calculated mean pore size. To have a better representation of the whole membrane structure, several SEM images from the various parts of the membrane cross-section were augmented to gather. Then the program package finds the best brightness that satisfies the mean pore size. Using several images help to include membrane heterogeneity in the PSD calculations. When the image contrast is fixed, the membrane porosity is calculated. The porosity is defined as the ratio of black area (the pore space) to the total area of the SEM image.

RESULTS AND DISCUSSION

Morphology Analysis

Figures 2 and 3 illustrate the SEM images of the fabricated membrane and their PSD. The smooth area within the PSD curvesis magnified to have a clear representation of the membrane porous structure.

As can be seen from Figures 2 and 3, when NMP is used as solvent, the membrane structure includes a thin layer with small pores and a porous sub-layer with finger type cavities. Porous layer has a thickness of 81.95 μm. However, the membrane that prepared with DMF solvent has sponge type structure. The reason behind the structural deference is refers to compatibility properties of solvent with non-solvent. In the case with the close compatibility of solvent and non-solvent, the phase inversion process occurs instantaneously whenthe polymer film enters in the coagulation bath. Consequently, porous structure with big pores forms. However, if solvent and non-solvent do not have a close compatibility, the phase inversion is slow and the membrane structure is sponge like.[1]

There is an increase in the pore size as the coagulation bath temperature increased. When NMP is used as the solvent, big macro voids are observed in the membrane structures that are prepared within the coagulation bath of 25 and 57°C. However, no void appears when the coagulation bath temperature was fixed at 8°C.

PSD curves give sharper peaks when NMP is used as the solvent. This means that the DMF-based membranes are more heterogeneous. In such cases, using a single SEM image for the analysis of the fabricated membranes may cause a considerable deviance from the real membrane properties. This is why several SEM images are used to predict the PSD curves.

Figure 2 shows that most of the pore's diameter is in the range of 0–5 μm when NMP is used as the solvent. Number of pores

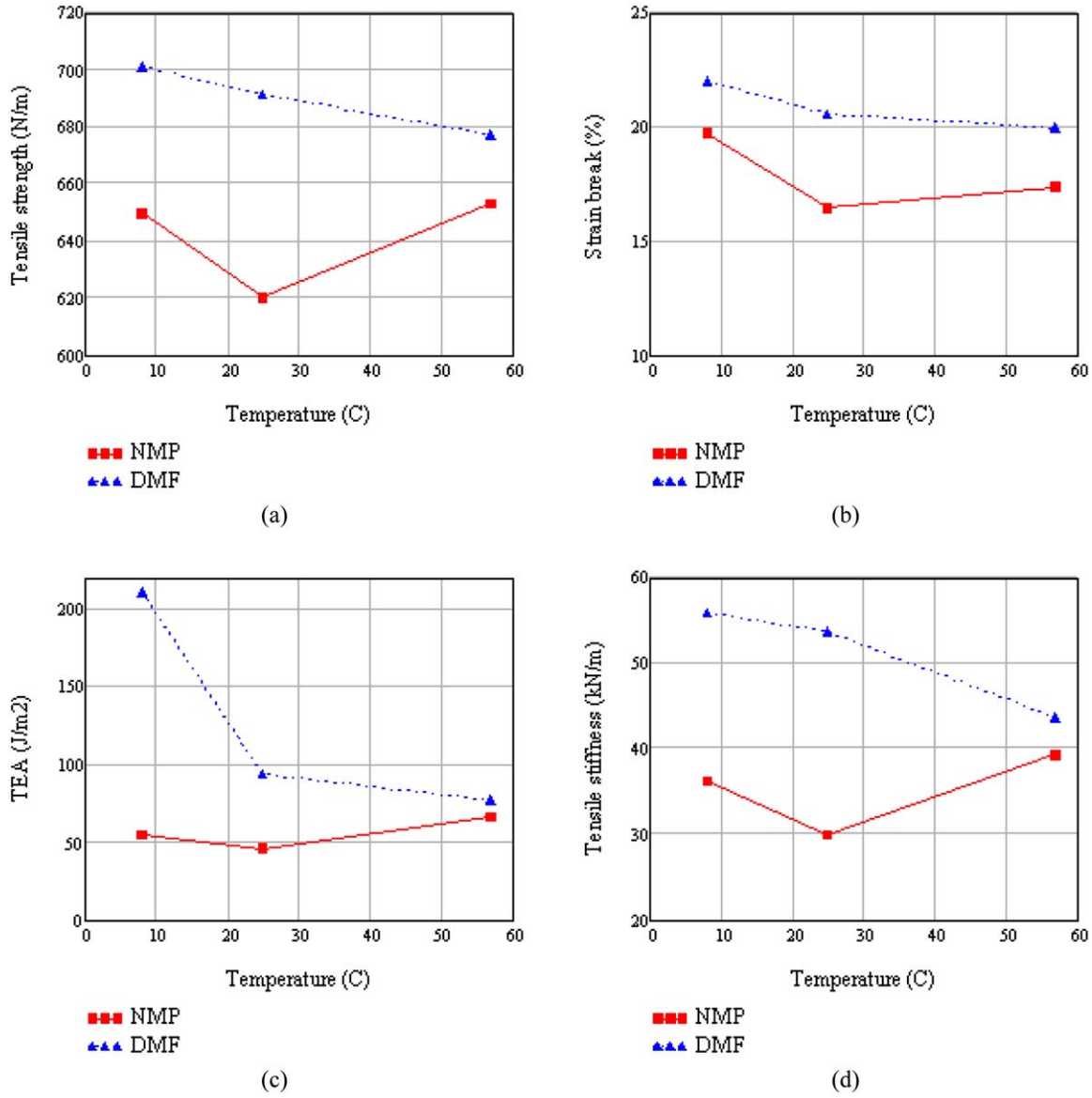

Figure 5. Mechanical properties of 20% of PSf membranes at 8, 25, and 57°C in NMP and DMF solvents. [Color figure can be viewed in the online issue, which is available at wileyonlinelibrary.com.]

is rapidly decreased with the increase of pore diameter above 5 μm. Maximum pore size is about 11 μm when the coagulation bath temperature was kept fixed in 8°C. On the other hand, the maximum pore diameters are near to 25 and 30 μm in the coagulation bath temperature of 25 and 57°C, respectively.

Figure 3 illustrates that for the membrane with the coagulation bath temperature of 25 and 57°C, most of the pores have diameters of 0–5 μm when DMF is used as the solvent. However, for the membrane that prepared in the coagulation bath temperature of 8°C, most of the pore diameters are less than 1 μm. The maximum pore size is about 6, 35, and 45 μm when the coagulation bath temperature is 8, 25, and 57°C, respectively.

The calculated mean pore size from gas permeability test is presented in Figure 4(a). In all temperature range of the coagulation bath, the mean pore size of the fabricated membrane is higher when NMP is used as solvent.The porosity of the membranes that are obtained from the image processing is showed in Figure 4(b). As can be seen the porosity values of the membranes with DMF solvent are less than the membranes with NMP solvent at all coagulation bath temperature.

As it is obvious from Figure 4, increasing in the coagulation bath temperature cause an increase in the membrane porosity. Such trend is also observed for the mean pore size when DMF is used as the solvent. However, the mean pore size curve passes through a maximum for the NMP-based membranes. Such behavior can be explained based on the SEM images and PSD that shown in Figure 2(a,b). PSD curve has sharper peak at the small pore regions for the coagulation bath temperature of 57°C. Therefore if a highly porous membrane with a finger shape structure is needed, the NMP should be used as the

solvent. However, to have a sponge like membrane with the lower mean pore size, DMF solvent should be used for the membrane fabrication.

Mechanical Properties

Membrane morphology and its mechanical properties depends on many factors such as composition of polymeric solutions (concentration ofpolymer, solvent, and additives), supporting materials, polymeric film thickness during the casting process, solvent and non-solvent characteristics, coagulation bath temperature, and the environmental conditions.[10,20]

According to an investigation on the synthetic parameter in the membrane formation process,[10,20] synthetic parameters increased by increasing in the coagulation bath temperature. There is a better interaction between the solvent and non-solvent which cause a quick phase inversion process. Therefore, the void space between the polymer molecules increased during the precipitation process. The membrane porous structure and in particular, the macro voids have a considerable effect on the mechanical characteristics of the synthetized membranes. Mechanical properties of the prepared membranes are shown in Figure 5.

As it can be seen from Figure 5, all of the PSf membranes made by NMP solvent have not adequate mechanical properties in compare to those made by DMF solvent. The reason behind such higher mechanical properties can be explained due to the higher coordination number of pores in the sponge like structure. In fact, mutual pore connectivity help to increase the mechanical strength.

There is a monotonous decrease in the mechanical properties of sponge like DMF-based membrane with the increase in the coagulation bath temperature. For instance, tensile energy absorbent (TEA) parameter at 57°C is 76.84 (J/m^2), while it is 93.39 (J/m^2) and 211.12 (J/m^2) for 25°C and 8°C, respectively. The reason could be caused as a result of existence of macro voids in the membrane porous structure. However, the mechanical properties curves pass through a minimum whenthe structure was finger like and NMP used as the solvent. On the other hand, except for the strain break, the NMP-based membranes have higher mechanical properties when they are prepared at the coagulation bath of 57°C.

Although mean pore size value of NMP-based membranes at the coagulation bath temperature of 8°C is much lower than those prepared in at the 57°C, the mechanical properties (such as tensile strength, TEA, and tensile stiffness) of 57°C membrane is higher. The results may cause by uniform porous structure of the membrane that prepared at the coagulation bath temperature of 57°C.

CONCLUSION

In this article, effect of coagulation bath temperature on the morphology and mechanical properties of polysulfone membranes are studied. Furthermore, a totally computerized image processing program package is developed to analyze the cross-sectional SEM images of the fabricated membranes. Pore size distribution and porosity of the fabricated membranes are determined using the proposed image processing procedure. The results showed that the new image processing procedure has a reasonable analysis of the membranes morphology and its structural properties. The following conclusion could be listed below:

- NMP-based membranes have finger-type structure while sponge-like structure observed when DMF is used as solvent. For both NMP and DMF solvents, membrane porosity increased when the coagulation bath temperature increased.
- By increase in the coagulation bath temperature, a monotonous increase in the mean pore size value of the DMF-based membranes is observed while the curve shows a maximum when NMP is used as solvent.
- DMF-based membranes have higher mechanical properties in compare to the NMP-based membranes. Also, mechanical properties decreased with rising of the coagulation bath temperature for DMF-based membranes. However, all mechanical properties passed through a minimum when NMP is used as solvent.
- Although DMF-based membranes have a heterogeneous pore size distribution, sharp peaks are observed in the region of small pores for NMP-based membranes.

REFERENCES

1. Tsai, H.; Li, L.; Wang, Y. C.; Li, C. L.; Huang, J.; Lai, J. Y. *J. Membr. Sci.* **2000**, *176*, 97.
2. Mulder, M. *Basic Principles of Membrane Technology*. Kluwer Academic Publishers: Dordrecht, **1991**.
3. Kaiser, V.; Stropnik, C.; Musil, V.; Brumen, M. *Eur. Polym. J.* **2007**, *43*, 2515.
4. Madaeni, S.; Rahimpour, A.; Barzin, J. *Iranian Polym. J.* **2005**, *14*, 421.
5. Guan, R.; Dai, H.; Li, C.; Liu, J.; Xu, J. *J. Membr. Sci.* **2006**, *277*, 148.
6. Iqbal, M.; Man, Z.; Mukhtar, H.; Dutta, B. K. *J. Membr. Sci.* **2008**, *318*, 167.
7. Shao, L.; Chung, T. S.; Wensley, G.; Goh, S. H.; Pramoda, K. P. *J. Membr. Sci.* **2004**, *244*, 77.
8. Wu, L.; Sunb, J.; Wang, Q. *J. Membr. Sci.* **2006**, *285*, 290.
9. Chun, K. Y.; Jang, S. H.; Kim, H. S.; Kim, Y. W.; Han, H. S.; Joe Y. *J. Membr. Sci.* **2000**, *169*, 197.
10. Chakrabarty, B.; Ghoshal, A. K.; Purkait, M. K. *J. Membr. Sci.* **2008**, *315*, 36.
11. Saljoughi, E.; Amirilargani, M.; Mohammadi, T. *Desalination* **2010**, *262*, 72.
12. Mohammadi, T.; Saljoughi, E. *Desalination* **2009**, *243*, 1.
13. Saljoughi, E.; Mohammadi, T. *Desalination* **2009**, *249*, 850.
14. Saljoughi, E.; Sadrzadeh, M.; Mohammadi, T. *J. Membr. Sci.* **2009**, *326*, 627.
15. Aroona, M. A.; Ismail, A. F.; Montazer-Rahmati, M. M.; Matsuura, T. *Separat. Purif. Technol.* **2010**, *72*, 194.
16. Chen, S.-H.; Liou, R.-M.; Lai, J.-Y.; Lai, C.-L. *Eur. Polym. J.* **2007**, *43*, 3997.

17. Barth, C.; Goncalves, M. C.; Pires, A. T. N.; Roeder, J.; Wolf, B. A.; *J. Membr. Sci.*, **2000**, *169*, 287.
18. Sobhanipoura, P.; Cheraghi, R.; Volinskyc, A. *Thermochim. Acta* **2011**, *518*, 101.
19. Barzin, J.; Madaeni, S. S.; Mirzadeh, H. *Iranian Polym. J.* **2005**, *14*, 353.
20. Chakrabarty, B.; Ghoshal, A. K.; Purkait, M. K. *J. Membr. Sci.* **2008**, *309*, 209.
21. Zheng, Q. Z.; Wang, P.; Yang, Y. N. *J. Membr. Sci.* **2006**, *279*, 230.
22. Conesa, A.; Gum′ı, T.; Palet, C. *J. Membr. Sci.* **2007**, *287*, 29.
23. Yang, B.; Manthiram, A. *J. Power Sources* **2006**, *153*, 29.
24. Bowen, W. R.; Doneva, T. A. *J. Membr. Sci.* **2000**, *171*, 141.
25. Zhao, C.; Zhou, X.; Yue, Y. *Desalination* **2000**, *129*, 107.
26. Sun, W.; Chen, T.; Chena, C.; Li, J. *J. Membr. Sci.* **2007**, *305*, 93.
27. Matsuyama, H.; Terammoto, M.; Nakatani, R.; Maki, T. *J. Appl. Polym. Sci.* **1999**, *74*, 171.
28. Buetehorna, S.; Koh, C. N.; Wintgens, T.; Volmering, D.; Vossenkaul, K.; Melin, T.; *Desalination* **2008**, *231*, 191.
29. Kim, I.; Lee, K. *J. Appl. Polym. Sci.* **2003**, *89*, 2562.
30. Deshmukh, S. P.; Li, K. *J. Membr. Sci.* **1998**, *150*, 75.